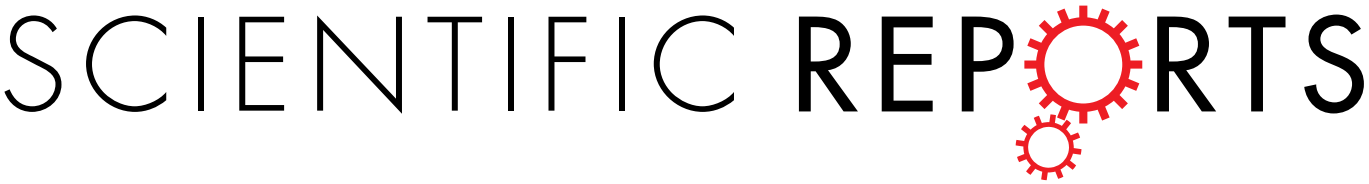

OPEN

# Conservation of the pure adiabatic state in Ehrenfest dynamics of the photoisomerization of molecules

Received: 28 May 2015
Accepted: 16 November 2015
Published: 11 December 2015

Yoshiyuki Miyamoto[1], Yoshitaka Tateyama[2,*], Norihisa Oyama[3,*] & Takahisa Ohno[3,*]

**We examined real-time-propagation time-dependent density functional theory (rtp-TDDFT) coupled with molecular dynamics (MD), which uses single-particle representation of time-evolving wavefunctions allowing exchange of orbital characteristics between occupied and empty states making the effective Kohn-Sham Hamiltonian dependent on the potential energy surfaces (PESs). This scheme is expected to lead to mean-field average of adiabatic potential energy surfaces (PESs), and is one of Ehrenfest (mean-field) approaches. However, we demonstrate that the mean-field average can be absent in simulating photoisomerization of azobenzene and ethylene molecules. A transition from the S2 to the S1 excited state without the mean- field average was observed after examining several rtp-TDDFT-MD trajectories of a photoexcited azobenzene molecule. The subsequent *trans-cis* isomerization was observed in our simulation, which is consistent with experimental observation and supported by previous calculations. The absence of the mean-field average of PESs was also observed for the transition between the S1 and S0 states, indicating that the MD simulation was on a single PES. Conversely, we found no transition to the ground state (S0 state) when we performed a MD simulation of an S1 excited ethylene molecule owing to the constraint on the occupation number of each molecular orbital. Thus, we conclude that, at least for azobenzene and ethylene molecules, the rtp-TDDFT-MD is an on-the-fly simulation that can automatically see the transition among the PESs of excited states without the mean-field average unless the simulation reaches the PES of the S0 state.**

MD simulations in electronic excited states are useful for photoinduced dynamics. A major problem in excited-state dynamics in materials is the transition among adiabatic potential energy surfaces (PESs). Based on the many-body wavefunction theory of quantum chemistry, the surface hopping approach[1–3] using multiple MD trajectories allowed excited-state dynamics to be studied by expressing the time-dependent electron wavefunctions as a linear combination of adiabatic wavefunctions with time-dependent coefficients. Because the Hamiltonian is common to molecular orbitals (MOs) no matter which PES the set of MOs belongs to, the transition matrix element can be computed directly. However, this approach becomes practically difficult as the size of molecules increases. This is because of the increase in the Slater-determinant size, the number of PESs involved in the transition, and the number of MD trajectories necessary for surface hopping operations, even when a single initial atomic configuration is used.

An alternative approach to the many-body wavefunction theory of quantum chemistry is density functional theory (DFT)[4,5] using the single-particle representation for wavefunctions of electrons with a Hamiltonian depending on the charge density of electrons. Combining surface-hopping with DFT is valid within linear-response time-dependent DFT (LR-TDDFT) that only considers the charge density of the electron ground state[6–9]. When the charge density depends strongly on PESs, the Kohn-Sham Hamiltonian should deviate from that of the ground state, meantime, the LR-TDDFT can follow the change of the self-consistent potential within linear response to the change of the charge[10].

On the other hand, an Ehrenfest approach[11] combined with real-time electron propagation by solving the time-dependent Schrödinger equation allows us to perform unbiased on-the-fly simulations of excited-state MD.

[1]Research Center for Computational Design of Advanced Functional Materials, National Institute of Advanced Industrial Science and Technology (AIST), Central 2, 1-1-1 Umezono, Tsukuba, Ibaraki 305–8568, Japan. [2]International Center for Materials Nanoarchitectonics (MANA), National Institute for Materials Science (NIMS), 1-1 Namiki, Tsukuba, Ibaraki 305-0044, Japan. [3]Computational Material Science Unit, National Institute for Materials Science (NIMS), 1-2-1 Sengen, Tsukuba, Ibaraki 305–0047, Japan. *These authors contributed equally to this work. Correspondence and requests for materials should be addressed to Y.M. (email: yoshi-miyamoto@aist.go.jp)

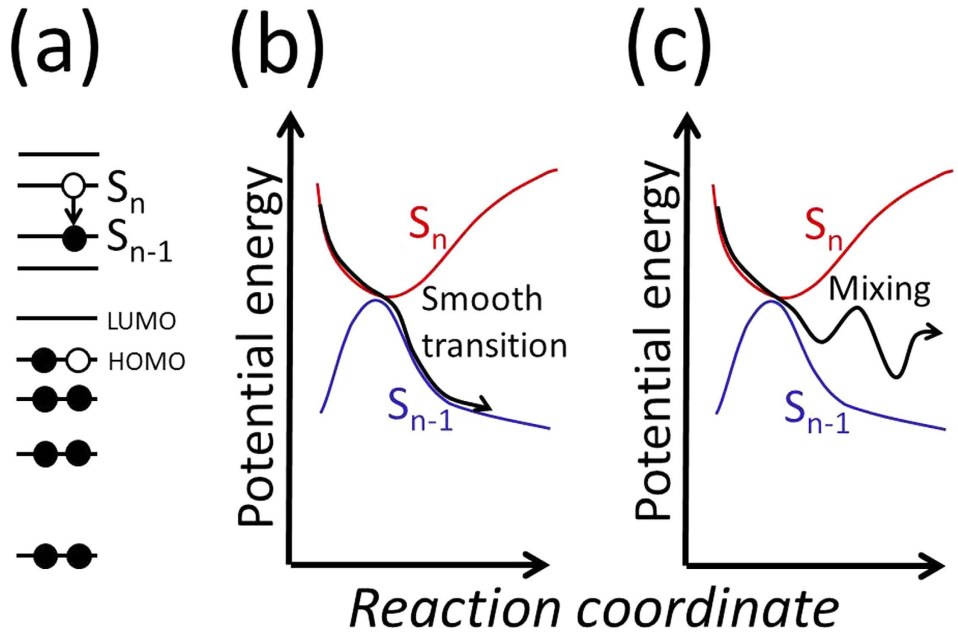


**Figure 1. Schematics of the $S_n \rightarrow S_{n-1}$ transition.** (**a**) Single-particle transition from the MO of the $S_n$ excited state to that of the $S_{n-1}$ excited state. (**b**) Transition and PES of the $S_n$ state to the PES of the $S_{n-1}$ state, and (**c**) Mean-field average of the $S_n$ and $S_{n-1}$ states throughout the simulation.

The transition among PESs is approximated as a mean-field average of several PESs, as discussed in ref. 2. Because real-time propagation time-dependent density functional theory (rtp-TDDFT)[12,13] coupled with MD is an Ehrenfest approach, the mean-field average of PESs is expected to arise. If so, the MD simulation is performed under the *mean* forces, and multiple MD trajectories are required.

Suppose we start from the singlet $S_n$ excited state of a molecule and experience the transition toward a singlet $S_{n-1}$ excited state. This transition is allowed without changing the set of occupation numbers of MOs by alternating the order of the energy levels of differently occupied MOs. Figure 1(a) shows this scenario with a schematic of a single-particle transition between two MOs. If the $S_n \rightarrow S_{n-1}$ transition occurs, rtp-TDDFT-MD should show the potential energy curve from the $S_n$ to the $S_{n-1}$ state (Fig. 1(b)). Otherwise, the rtp-TDDFT-MD shows the mean-field average of the $S_n$ and $S_{n-1}$ states by taking the intermediate value of the potential (Fig. 1(c)).

In this paper, we examined the rtp-TDDFT-MD approach to photoexcited molecular systems to determine which of the scenarios in Fig. 1(b,c) occurs. We chose practical, common examples. The first case is photoinduced $S_2$ excitation and transition to the $S_1$ state in azobenzene and subsequent *trans-cis* isomerization. The other case is an $S_1$ excited ethylene ($C_2H_4$) molecule for examining the $S_1$ to $S_0$ transition. For both cases, we did not see the mean-field average shown in Fig. 1(b). Azobenzene undergoes a smooth $S_2 \rightarrow S_1$ transition, whereas $C_2H_4$ shows no $S_1 \rightarrow S_0$ transition. Thus, we conclude that, at least for the current cases, the rtp-TDDFT-MD is an on-the-fly tool to model the PES transition automatically unless the simulation reaches the PES of the $S_0$ state. (Note that the current scheme did not show the decay into the ground state.).

## Computational schemes

To examine the presence or absence of the mean-field average of PESs in the rtp-TDDFT-MD simulation, we used the local density approximation (LDA)[14] for the adiabatic exchange-correlation functional of DFT. The LDA was used because there are previous studies of azobenzene[15] that show that PESs for the $S_0$, $S_1$, and $S_2$ states obtained with several types of DFT exchange-correlation functional, such as the BLYP[16,17] and PBE functional[18] of the generalized gradient approximation and LDA, are similar to each other, and to those obtained by the many-body wavefunction theory of quantum chemistry with a higher level of accuracy including the complete active space self-consistent field (CASSCF) method[19]. LDA also performed well for the photoinduced reaction of diazomethane, which is a precursor of carbene[20] and the $S_1$ excited-state MD of $C_2H_4$ presented in this work, which is consistent with ref. 21.

The calculation was performed by using plane-wave total energy formalisms[22] and the norm-conserving pseudopotentials[23]. The cutoff energy for the plane-wave basis set was set as 60 Ry. The rtp-TDDT-MD simulation was performed by using the code developed in ref. 24. The real-time propagation of the electron wavefunctions by solving the time-dependent Kohn-Sham equation,

$$i\hbar \frac{\partial \psi_n^{KS}(\mathbf{r}, t)}{\partial t} = H^{KS}(\rho(\mathbf{r}, t))\psi_n^{KS}(\mathbf{r}, t), \quad (1)$$

was computed by applying the Suzuki-Trotter split operator method[25,26] with a time-step interval of 0.03 a.u. (1 a.u. $= 2.42 \times 10^{-2}$ fs). Here, $\psi_n^{KS}(\mathbf{r}, t)$ is the $n$-th time-dependent Kohn-Sham orbital and $H^{KS}(\mathbf{r}, t)$ is the Kohn-Sham Hamiltonian of TDDFT[12]. $\rho(\mathbf{r}, t)$ is the electron charge density consisting of the norm of all occupied

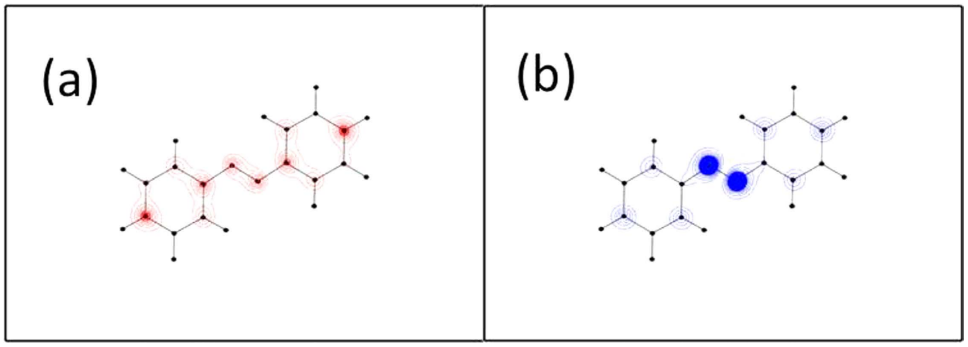


**Figure 2. Contour maps of norms of (a) HOMO-1 and (b) LUMO states of an azobenzene molecule.** The contour line interval is set as 0.019 $e/Å^3$, which is also a common minimum value of the contour lines in (**a**,**b**).

Kohn-Sham orbitals. To perform the MD simulations, forces were derived from the same formalism as the Hellmann-Feynman force for the plane wave scheme[22]. To prepare the excited state, we manually set occupation numbers of some MOs as half and performed the self-consistent calculation as in ref. 27 within the constraint DFT (ΔSCF) scheme. The validation of using the ΔSCF scheme has been discussed thoroughly and is summarized in ref. 28, and agreement with PES by TDDFT was reported for azobenzene in ref. 15. We employed a spin-unpolarized approximation, assuming that half-occupied MOs consist of 0.5 electrons with an up spin and 0.5 electrons with a down spin.

## Results for azobenzene

**Optical and orbital properties.** First, we optimized the molecular structure of azobenzene in the electronic ground state. The cell size was $20 \times 14 \times 14\,Å^3$ with the longest lattice vector parallel to the long molecular axis of azobenzene. We assumed no symmetric restriction in determining the atomic coordinates and the electron charge density of azobenzene. Atomic coordinates include an error of $\pm 0.042$ Å that was derived from the averaged deviation in equivalent atomic pairs of an azobenzene molecule after $C_2$ rotation around the center of the N = N bond. The optimized atomic coordinates are listed in Table S1 in the supplementary material. According to the optical matrix elements obtained by using the Kohn-Sham orbital from *static* LDA calculations, the magnitude of the oscillator strength for the $S_2$ excitation is stronger than the $S_1$ excitation. The corresponding excitation energies for the $S_1$ and $S_2$ excitations are 2.48 and 3.37 eV, respectively, obtained by a Fourier transformation of the dipole dynamics induced by a short pulse[29,30] based on rtp-TDDFT. These quantities are comparable to experimental data[31] with an error of ~0.3 eV for $S_1$ and ~0.7 eV for $S_2$.

The HOMO-1 and LUMO orbitals individually have N-N $\pi$ and $\pi^*$ characters, as shown by the contour maps of the norm of each MO in Fig. 2. These orbital characters obtained by LDA are consistent with theoretical natural orbital plots that were obtained by the CASSCF method[32].

**rtp-TDDFT-MD electron-ion dynamics.** The rtp-TDDFT-MD simulations of azobenzene were performed with no symmetry constraints. At the beginning of the rtp-TDDFT-MD simulation, all ions had no initial velocities. We used four initial conditions, one of which was the optimized atomic geometry and others were obtained by sampling the atomic geometries of snapshots of a single trajectory of the ground-state MD simulation. The initial condition of the MD simulation was assumed with randomized ionic velocities with a corresponding temperature of 230 K. The four initial atomic coordinates are listed in Tables S1 to S4 in the supplementary materials with a potential energy variation of up to 0.5 eV per azobenzene molecule.

We compared the potential energy of the rtp-TDDFT-MD simulation

$$\begin{aligned} E_{\mathrm{tot}}(t) \;=\; & \sum_n f_{\mathrm{n}}\Big[\int \psi_{\mathrm{n}}^{KS*}(\mathbf{r},\,t)\frac{-1}{2}\Delta\psi_{\mathrm{n}}^{KS}(\mathbf{r},\,t)\,d\mathbf{r} \\ & + \iint \psi_{\mathrm{n}}^{KS*}(\mathbf{r},\,t)\,V_{nonloc}^{ps}(\mathbf{r},\,\mathbf{r}')\,\psi_{\mathrm{n}}^{KS*}(\mathbf{r}',\,t)\,d\mathbf{r}d\mathbf{r}'\Big] \\ & + \frac{1}{2}\iint \frac{\rho(\mathbf{r},\,t)\,\rho(\mathbf{r}',\,t)}{|\mathbf{r}-\mathbf{r}'|}d\mathbf{r}d\mathbf{r}' + \int \varepsilon_{XC}[\rho(\mathbf{r},\,t)]\,\rho(\mathbf{r},\,t)\,d\mathbf{r} \\ & + \sum_I Z_I \int \frac{\rho(\mathbf{r},\,t)}{|\mathbf{r}-\mathbf{R}_I(t)|}d\mathbf{r} + \sum_{I\neq J}\frac{Z_I Z_J}{|\mathbf{R}_I(t)-\mathbf{R}_J(t)|} \end{aligned} \tag{2}$$

with the potential energy obtained by *static* DFT, which is also expressed by equation (2), but without $t$ dependence. In these four rtp-TDDFT-MD trajectories, sets of coordinates obtained from several snapshots were used to calculate the potential by *static* DFT for the ground state, and $S_1$ and $S_2$ excited states within the ΔSCF scheme. In equation (2), $\frac{-1}{2}\Delta$ is the kinetic-energy operator. $V_{nonloc}^{ps}$ is the sum of the non-local terms of the pseudopotentials. $f_{\mathrm{n}}$ is the occupation number, which was manually set for excited states. $\varepsilon_{XC}$ is the exchange-correlation potential as a functional of the charge density. $Z_I$ and $\mathbf{R}_I$ are the charge and coordinate of the $I$-th ion, respectively.

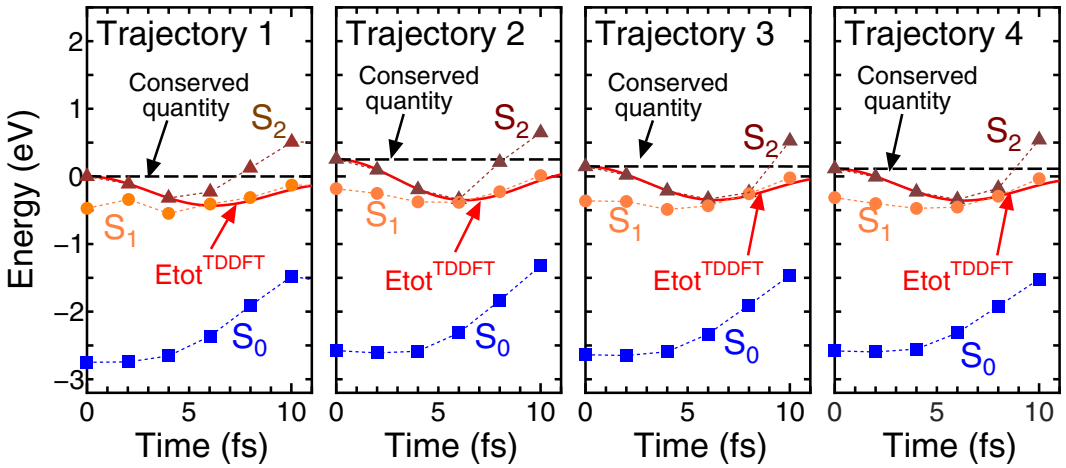


**Figure 3. Comparison of the TDDFT potential energy and *static* DFT potential energies of $S_n$ states with $n = 0,1$, and 2 for four trajectories of the rtp-TDDFT-MD simulation.** Hatched triangles, circles, and squares are the total energies of the $S_2$, $S_1$, and $S_0$ states, respectively, obtained by *static* DFT with common atomic coordinates in the snapshot of the rtp-TDDFT-MD simulations. The origin of the potential is set to that of the $S_2$ state at beginning of "Trajectory 1".

By setting the $S_2$ excited state as an initial condition, the rtp-TDDFT simulations were continued to 11 fs, which induced the $S_2 \rightarrow S_1$ transition, as described later. Figure 3 shows the results for the time-evolution of the rtp-TDDFT potential energy of the four trajectories, in which $E_{\mathrm{TOT}}^{\mathrm{TDDFT}}$ is the potential energy obtained by equation (2) throughout the rtp-TDDFT-MD simulations. Solid squares, circles, and triangles show the potential energies of $S_0$, $S_1$, and $S_2$ states obtained by the *static* DFT at the atomic coordinates for the corresponding times determined by the rtp-TDDFT-MD simulations. For all trajectories, the potential energy obtained by the rtp-TDDFT-MD simulation followed the PES of the $S_2$ state at the beginning then switched to that of the $S_1$ state after 6 fs, which indicates that the lifetime of the $S_2$ state is short. (One can note that the $E_{\mathrm{TOT}}^{\mathrm{TDDFT}}$ is in midpoint between $S_2$ and $S_1$ state from 4 fs to 6 fs in "Trajectory 1" of Fig. 3 but follows $S_1$ state later than 6 fs. In such a short time-constant, the influence on ionic motion is negligibly small, thus MD simulation will follow a trajectory of $S_1$ state later than 6 fs).

Even at the transition from the $S_2$ to the $S_1$ states, the original orbital characters of HOMO-1 and LUMO remained as same as those displayed in Fig. 1(a,b). However, the expectation values of the Kohn-Sham Hamiltonian for HOMO-1 and HOMO, which can be approximately interpreted as energy levels, alternated after 6 fs, which was consistent with the orbital character of the $S_1$ state obtained by ΔSCF. This indicates that the change in the level ordering of the MO at particular atomic coordinates can automatically be searched by the rtp-TDDFT-MD simulation. The automatic on-the-fly identification of PES-crossing is an important advantage of the rtp-TDDFT-MD simulation.

Finally in this subsection, we show that Fig. 3 indicates that the value of the potential energy obtained by the rtp-TDDFT-MD simulation does not show the intermediate value between those of the $S_1$ and $S_2$ states. Thus, we conclude that the mean-field average of PESs is not the case in the rtp-TDDFT-MD simulation of $S_2$ excited azobenzene. The slight deviation in the values of the potentials in Fig. 3 may arise from a small amount of mixing between the $S_1$ and $S_0$ states, which is negligible considering the photoisomerization dynamics presented in the next subsection.

**Long-time simulation of photoisomerization.** The fact that rtp-TDDFT-MD beyond 6 fs follows a pure $S_1$ state can also be demonstrated by a long-time simulation of the *trans-cis* photoisomerization of azobenzene. Because this long-time simulation is computationally expensive, we have chosen only "Trajectory 1" in Fig. 3 as a sample case. Figure 4(a) shows a conformational change in azobenzene in the long-time simulation. Up to 250 fs, the N = N axis started to move away from the molecular plane in the direction denoted by the blue arrow, and then at 250 fs two benzene rings began to lift from the original molecular plane. This is the beginning of the rotation pathway toward *cis*-azobenzene, which was achieved at $t \sim 500$ fs in the simulation. This time constant is the same order of magnitude as the constant obtained by the time-variation of the fluorescence data[33,34], the energy-broadening factors of which indicate a lifetime of 200–700 fs. Statistical treatment of many trajectories of electron-ion dynamics including energy dissipation processes would be necessary for precise comparison, which is beyond the scope of the current work. We confirmed the (meta)stability of the last geometry of *cis*-azobenzene by performing conjugate-gradient geometry optimization in the $S_0$ state (electronic ground state). The computed total energy of the *cis*-azobenzene is 0.8 eV higher than *trans*-azobenzene in the $S_1$ state within the LDA level of accuracy.

We also compared our current results with recent simulations of azobenzene[35–39]. Non-adiabatic transitions using surface hopping technique within fewest-switch scheme were done by Ref. 35,39, while others[36–38] studied profiles of PESs of excited states. Grannuci *et al.*[35] reported a short time constant for both the $S_2 \rightarrow S_1$ transition and the subsequent rotation pathway of the photo-isomerization within sub ps, which is consistent with our current results for photo-isomerization despite the different theoretical approach in ref. 35, *i.e.*, a combination of CASSCF

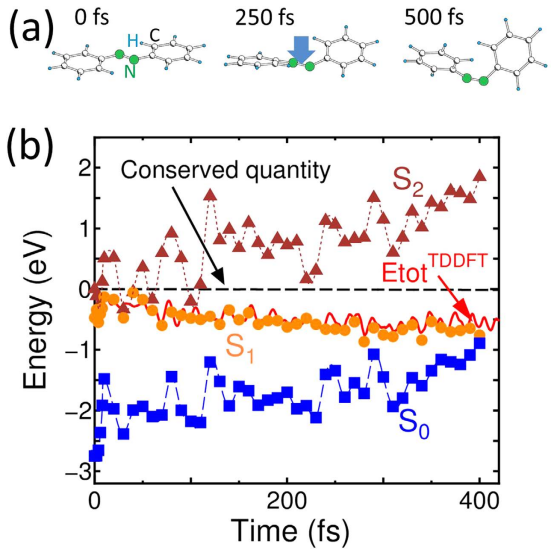


**Figure 4.** (**a**) Conformations of an azobenzene molecule at $t = 0$, 250, and 500 fs. Large green circles, small blue hatched circles, and open circles denote nitrogen, hydrogen, and carbon atoms, respectively. The vertical blue arrow denotes the initial motion of the N = N axis being pushed down out of the molecular plane. (**b**) Potential energy calculated by rtp-TDDFT-MD (solid red line) throughout the *trans-cis* conversion of an azobenzene molecule upon $S_2$ excitation. Hatched triangles, circles, and squares denote *static* DFT total energies of $S_2$, $S_1$, and $S_0$ states, respectively. The origin of the potential is set as that of the $S_2$ state at $t = 0$ fs. The dashed line denotes the conserved quantity, and the potential energy plus kinetic energies of all ions.

and surface hopping with fewest switching mode. Meantime, the time constant around 6 fs for $S_2 \rightarrow S_1$ transition in current simulation cannot be directly compared with ref. 35 because of the fewest-switch scheme. Other theoretical works[36,37] using CASSCF[19] formalisms and B3LYP[16,17,40] functionals, showed the absence of a reaction barrier along with the rotational pathway and presence of the barrier along with inversion pathways upon $S_1$ excitation. The current on-the-fly simulation starting from $S_2$ excitation through relaxation to $S_1$ excitation also shows no barrier for the rotational pathway, as seen in the potential-time plots in Figs 3 and 4(b). However, inversion pathways for photoisomerization that contradict our results have also been reported[38,39]. Theoretical conclusions about the pathway of photoisomerization are still under debate. However, this problem does not affect our current conclusion concerning the conservation of pure adiabatic states in the Ehrenfest dynamics because the potential mixing should be concerned only at a conformation region of the "cis"-azobenzene.

The oscillating behaviour in the potential in Fig. 4(b) arises from the induction of many vibration modes in the azobenzene molecule, such as bond stretching and bending, throughout the *trans-cis* conversion. During the isomerization, we monitored the N = N bond length as a function of time. Figure 5(a) shows the computed value and Fig. 5(b) shows its Fourier transformation in wavenumber domains. The Fourier transformation of the time-evolution of the N = N length shows two major peaks at 1414 and 1145 $cm^{-1}$, which are consistent with the Raman spectra of photoexcited azobenzene at 1428 and 1130 $cm^{-1}$[34] within the possible error caused by LDA. These peaks are also consistent with recent theoretical work with higher accuracies in many-body treatments[32,41] indicating the preservation of the double bond character of the N = N axis.

The potential energy obtained by the rtp-TDDFT-MD simulation in Fig. 4(b) was compared with those obtained by *static* DFT calculations of $S_2$, $S_1$, and $S_0$ states along with the MD-trajectory. The long-time simulation showed that the potential of the rtp-TDDFT-MD simulation follows that of the $S_1$ state instead of showing the mean-field average of PESs, and the potential goes near the $S_0$ state after 400 fs.

**Results for the $C_2H_4$ molecule.** The simulation in Fig. 4(b) could demonstrate the $S_1 \rightarrow S_0$ transition or mean-field average of these states. However, examining azobenzene is too time-consuming because it is expected that the time-constant for the intersections of PESs of the $S_1$ and $S_0$ states will be beyond 500 fs at all MD-trajectories. We chose another common molecule, $C_2H_4$, which has $\pi$ and $\pi^*$ orbitals equivalent to a 90° twist of the two $CH_2$ components of the $C_2H_4$ molecule, which is similar to azobenzene photoisomerization.

Figure 6(a) shows the dynamics of the $C_2H_4$ molecules under $S_1$ excitation. The initial atomic configuration was slightly twisted from the optimized structure under a periodic $10 \times 5 \times 5$ $Å^3$ box. The coordinates are listed in Table S5 in the supplementary material. There are three $C_2$ axes; one of the three is along the C-C bond axis and the other two are perpendicular to the C-C axis. The three $C_2$ axes remain, even during photoisomerization of a $C_2H_4$ molecule keeping a constraint under the $D_2$ symmetry. Assuming no initial velocities on all atoms, the molecule immediately shows the rotation of the $CH_2$ unit being accompanied by C-C stretching. Even within the LDA functional, the dynamics are consistent with quantum chemistry many-body wavefunction theory coupled with a surface-hopping technique[21]. Ben-Nun *et al.*[21] also present further results for the intramolecular proton transfer derived from a lower symmetric configuration, which is beyond the scope of our work.

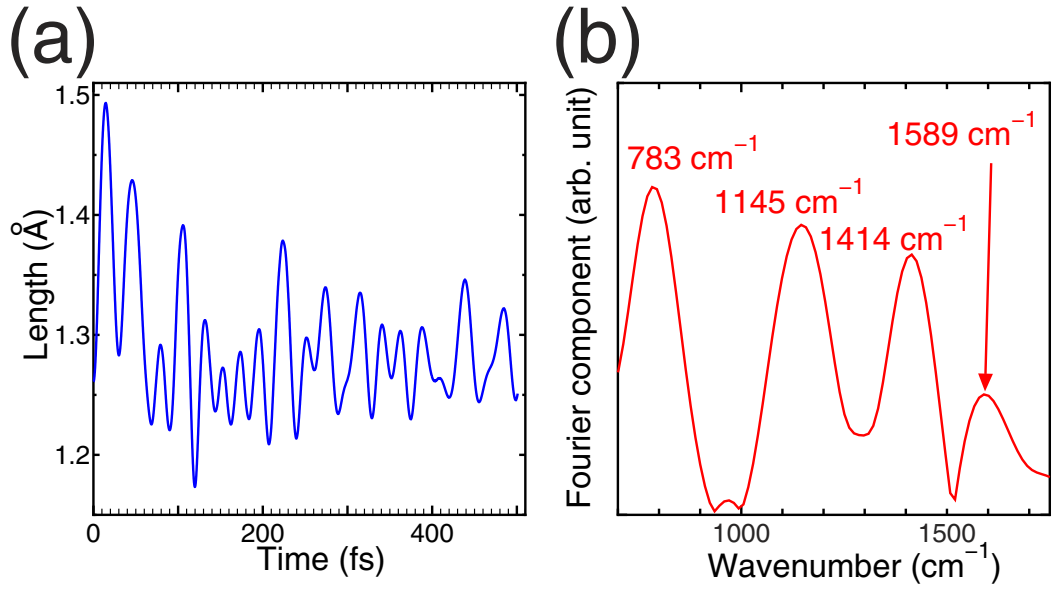


**Figure 5.** (**a**) Time-evolution of the N = N length of the azobenzene molecule throughout the dynamics displayed in Fig. 4. (**b**) Period domain of N = N stretching after the data in Fig. 5 (**a**) has been Fourier transformed. The corresponding wavenumbers expressing the frequencies are also displayed.

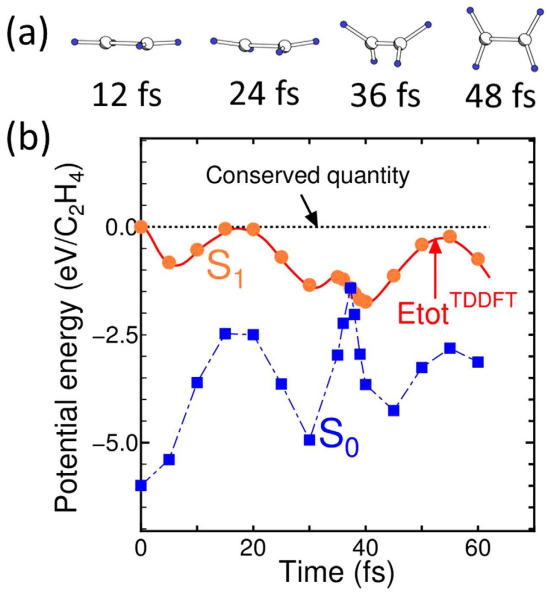


**Figure 6.** (**a**) Dynamics of a $C_2H_4$ molecule upon $S_1$ excitation under high geometric symmetry conditions. (**b**) Corresponding potentials of the rtp-TDDFT-MD simulation and *static* DFT for the $S_1$ and $S_0$ states. Hatched squares and circles denote *static* DFT total energies of the $S_0$ and $S_1$ states, respectively.

Figure 6(b) shows a comparison of the potential energies obtained by ftp-TDDFT-MD and by *static* DFT for the $S_1$ and $S_0$ states. The simulation showed the intersection of PESs of the $S_1$ and $S_0$ states. Similar to the azobenzene simulation, the mean-field average of the PESs did not occur. The potential energy of rtp-TDDFT-MD coincided with the PES of the $S_1$ state, and thus the $S_1 \rightarrow S_0$ transition was inhibited. Considering the orbital occupation, the $S_0$ state does not have a half-occupied MO, so a smooth transfer maintaining the numbers of fully and half-occupied MOs did not occur. We also examined the inhibition of the $S_1 \rightarrow S_0$ transition and the mean-field average in the $C_2H_4$ molecule with no symmetric restriction on three MD trajectories. For the trajectories, see Tables S6 to S8 in the supplementary information, which show the initial conditions in the atomic coordinates and velocities of ions randomly distributed with a corresponding temperature of about 110 K. Here, the calculations were performed with a $10 \times 10 \times 10$ Å$^3$ periodic box. The results are displayed in Fig. 7, where the intersection of $S_1$ and $S_0$ can be seen several times in all trajectories.

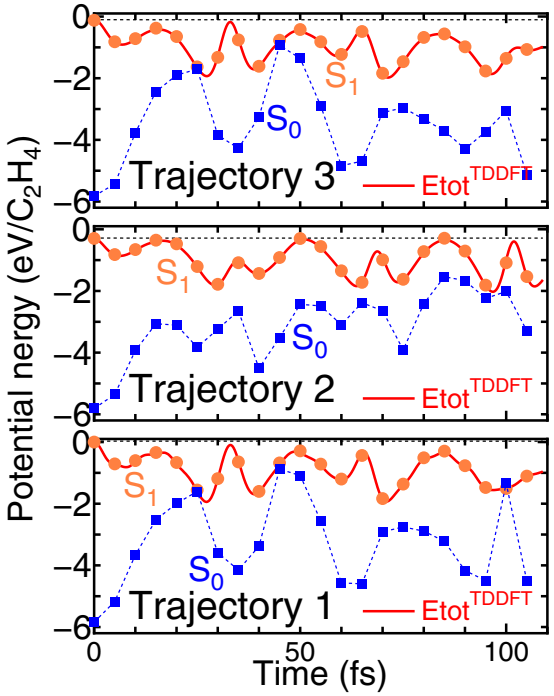


**Figure 7. Potential energies on the three non-symmetric trajectories for the rtp-TDDFT-MD simulation of the $S_1$ excited $C_2H_4$ molecule.** Potential energies computed by *static* DFT for $S_1$ and $S_0$ states are also displayed. Hatched squares and circles denote *static* DFT total energies of the $S_0$ and $S_1$ states, respectively. The origin is set as the potential energy of the $S_1$ state at the beginning of "Trajectory 1".

If the spin-polarized Kohn-Sham wavefunction is available, the $S_1$ state can be expressed with a singly occupied LUMO and HOMO with up and down spins, respectively. If the time-evolution of the spin-up LUMO smoothly changes the orbital into a spin-up HOMO when the PESs of the $S_1$ and $S_0$ states intersect, the smooth $S_1 \rightarrow S_0$ transition can be simulated. However, this is still not trivial in the rtp-TDDFT-MD scheme because there can also be an opposite change in wavefunction, namely changing the spin-down HOMO into a spin-down LUMO. If this occurs, we re-create an $S_1$ state with the opposite spin configuration. Therefore, we expect that a smooth $S_1 \rightarrow S_0$ transition is not guaranteed with the spin-polarized rtp-TDDFT-MD approach.

**Concluding remarks.** The absence of the mean-field average of PESs may only occur in cases allowing neither charge transfer nor molecular disintegration. When disintegration occurs in the rtp-TDDFT-MD simulation, the numbers of distributed electrons are likely to be fractional. In this case, the simulation should be under a mean-field average of many PESs, in contrast to our present results. This case was also discussed in ref. 2.

However, the presence of many MOs may also explain the absence of the mean-field average particularly in current cases of rtp-TDDFT-MD. A $C_2H_4$ molecule has seven occupied MOs per spin for the $S_1$ excited state within $\Delta$SCF, whereas an azobenzene molecule has 35 occupied MOs per spin for $S_2$ excited states. This number of MOs can interfere with each other through the Hartree-exchange-correlation potential of DFT during the rtp-TDDFT-MD simulation. This contradicts the two PES systems with a coherent Rabi-oscillation expressing the mean-field average of PESs. The interference becomes substantial as the number of wavefunctions increases and can suppress the mean-field average of PESs, setting the probability weighted on a particular PES. Interference among many orbitals is also seen in extended systems, similar to the relaxation of hot carriers in carbon nanotubes[42].

In summary, we have demonstrated the absence of the mean-field average of PESs throughout the rtp-TDDFT-MD simulations for photoexcited azobenzene and $C_2H_4$ molecules. The $S_2 \rightarrow S_1$ transition in azobenzene was observed in several trajectories followed by the *trans-cis* isomerization, which was consistent with previous experimental and theoretical studies. Conversely, the $S_1 \rightarrow S_0$ transition was not observed in an $S_1$ excited $C_2H_4$ molecule owing to the restriction of occupation numbers. Therefore, we concluded that each MD trajectory presented here was on a single PES and that the rtp-TDDFT-MD approach, at least for the current cases, is an on-the-fly tool for automatically monitoring transitions among PESs, unless the simulation reaches the PES of the $S_0$ state. Further investigation of other molecules will help to generalize our findings.

## References

1. Tully, J. C. & Preston, R. K. Trajectory surface hopping approach to nonadiabatic molecular collisions: The reaction of roman $h^+$ with roman $d_2$. *J. Chem. Phys.* **55,** 562–572 (1971).
2. Tully, J. C. Molecular dynamics with electronic transitions. *J. Chem. Phys.* **93,** 1061–1071 (1990).
3. Parandekar, P. & Tully, J. C. Mixed quantum-classical equilibrium. *J. Chem. Phys.* **122,** 094102 (2005).
4. Hohenberg, P. & Kohn, W. Inhomogeneous electron gas. *Phys. Rev.* **136,** B864–871 (1964).
5. Kohn, W. & Sham, L. Self-consistent equations including exchange and correlation effects. *Phys. Rev.* **140,** A1133–A1138 (1965).

6. Craig, C. F., Duncan, W. R. & Prezhdo, O. V. Trajectory surface hopping in the time-dependent kohn-sham approach for electron-nuclear dynamics. *Phys. Rev. Lett* **95,** 163001 (2005).
7. Maitra, N. T. On correlated electron-nuclear dynamics using time-dependent density functional theory. *J. Chem. Phys* **125,** 014110 (2006).
8. Tapavicza, E., Tavernelli, I. & Rothlisberger, U. Trajectory surface hopping within linear response time-dependent density-functional theory. *Phys. Rev. Lett* **98,** 023001 (2007).
9. Curchod, B. F. E., Rothlisberger, U. & Tavernelli, I. Trajectory-based nonadiabatic dynamics with time-dependent density functional theory. *ChemPhysChem* **14,** 1314 (2013).
10. Hutter, J. Excited state nuclear forces from the tamm-dancoff approximation to time-dependent density functional theory within the plane wave basis set framework. *J. Chem. Phys.* **118,** 3928–3934 (2003).
11. Ehrenfest, P. Remark about the approached validity of the classic mechanics within the quantum mechanics. *Z. Phys.* **45,** 455–457 (1927).
12. Runge, E. & Gross, E. K. U. Density-functional theory for time-dependent systems. *Phys. Rev. Lett* **52,** 997–1000 (1984).
13. Edited *et al.* Fundamentals of time-dependent density functional theory. In *Lecture Note of Physics* vol. 837 (Springer, Berlin, 2012).
14. Perdew, J. P. & Zunger, A. Self-interaction correction to density-functional approximation for many-electron systems. *Phys. Rev. B* **23,** 5048–5079 (1981).
15. Maurer, R. J. & Reuter, K. Assessing computationally efficient isomerization dynamics: $\delta$scf density-functional theory study of azobenzene molecular switching. *J. Chem. Phys* **135,** 224303 (2011).
16. Becke, A. D. Density-functional exchange-energy approximation with correct asymptotic behavior. *Phys. Rev. A* **38,** 3098–3100 (1988).
17. Lee, C., Yang, W. & Parr, R. G. Development of the colle-salvetti correction-energy formula into a functional of the electron density. *Phys. Rev. B* **37,** 785–789 (1988).
18. Perdew, J. P., Burke, K. & Ernzerhof, M. Generalized gradient approximation made simple. *Phys. Rev. Lett.* **77,** 3865–3868 (1996).
19. Roos, B. O., Taylor, P. R. & Siegbahn, P. E. M. A complete active space scf method (casscf) using a density matrix formulated super-ci approach. *Chem. Phys.* **48,** 157–173 (1980).
20. Lee, H., Miyamoto, Y. & Tateyama, Y. Excited state carbene formation from uv irradiated diazomethane. *J. Org. Chem.* **74,** 562–567 (2008).
21. Ben-Nun, M. & Martínez, T. J. Photodynamics of ethylene: ab initio studies of conical intersections. *Chem. Phys.* **259,** 237–248 (2000).
22. Ihm, J., Zunger, A. & Cohen, M. L. Momentum space formalism for the total energy of solids. *Phys. C: Solid State Physics* **12,** 4409–4422 (1979).
23. Troullier, N. & Martins, J. L. Efficient pseudopotentials for plane-wave calculations. *Phys. Rev. B* **43,** 1993–2006 (1991).
24. Sugino, O. & Miyamoto, Y. Density-functional approach to electron dynamics: Stable simulation under a self-consistent field. *Phys. Rev. B* **59,** 2579–2586 (1999).
25. Suzuki, M. General nonsymmetric higher-order decompposition of exponential operators and symplectic integration. *J. Phys. Soc. Jpn* **61,** 3015–3019 (1992).
26. Suzuki, M. & Yamauchi, T. Convergence of unitary and complex decompositions of exponential operators. *J. Math. Phys* **34,** 4892–4897 (1993).
27. Tiago, M. L., Ismail-Beigi, S. & Louie, S. G. Photoisomerization of azobenzene from first-principles constrained density-functional calculations. *J. Chem. Phys.* **122,** 094311 (2005).
28. Onida, G., Reining, L. & Rubio, A. Electronic excitations: density-functional versus many-body green's-function approaches. *Rev. Mod. Phys.* **74,** 601–659 (2002).
29. Yabana, K. & Bertsch, G. F. Time-dependent local-density approximation in real time. *Phys. Rev. B* **54,** 4484–4487 (1996).
30. Castro, A. *et al.* Octopus: a tool for the application of time-dependent density functional theory. *Phys. Stat. Solid B* **243,** 2465–2488 (2006).
31. Andersson, J., Petterson, R. & Tegnér, L. Flash photolysis experiments in the vapor phase at elevated temperatures i: Spectra of azobenzene and the kinetics of its thermal cis-trans isomerization. *J. Photochem* **20,** 17–32 (1982).
32. Harabuchi, Y., Ishii, M., Nakayama, A., Noro, T. & Taketsugu, T. A multireference perturbation study of the nn stretching frequency of trans-azobenzene $n\pi\pi^*$ excitation and an implication for the photoisomerization mechanisms. *J. Chem. Phys.* **138,** 064305 (2013).
33. Fujino, T., Arzhantsev, S. Y. & Tahara, T. Femtosecond time-resolved fluorescence study of photoisomerization of trans-azobenzene. *J. Phys. Chem. A* **105,** 8123–8129 (2001).
34. Fujino, T., Arzhantsev, S. Y. & Tahara, T. Femtosecond/picosecond time-resolved spectroscopy of trans-azobenzene: Isomerization mechanism following $s_2(\pi\pi^*) \leftarrow s_0$ photoexcitation. *Bull. Chem. Soc. Jpn.* **75,** 1031–1040 (2002).
35. Granucci, G. & Persico, M. Excited state dynamics with the direct trajectory surface hopping method: azobenzene and its derivatives as a case study. *Theor. Chem. Acc.* **117,** 1131 (2007).
36. Diau, E. W.-G. A new trans-to-cis photoisomerization mechanism of azobenzene on the $s_1(n, \sigma^*)$ surface. *J. Phys. Chem. A* **108,** 950–956 (2004).
37. Crecca, C. R. & Roitberg, A. E. Theoretical study of the isomerization mechanism of azobenzene and disubstituted azobenzene derivatives. *J. Phys. Chem. A* **110,** 8188–8203 (2006).
38. Schultz, T. *et al.* A. mechanism and dynamics of azobenzene photoisomerization. *J. Am. Chem. Soc.* **125,** 8098–8099 (2003).
39. Yu, L., Xuac, C. & Zhu, C. Probing the $\pi$-$\pi^*$ photoisomerization mechanism of *cis*-azobenzene by multi-state *ab initio* on-the-fly trajectory dynamics simulation. *Phys. Chem. Chem. Phys.* **17,** 17646 (2015).
40. Becke, A. D. Density functional thermochemistry. iii. the role of exact exchange. *J. Chem. Phys.* **98,** 5648–5652 (1993).
41. Gagliardi, L., Orlandi, G., Bernardi, F., Cembran, A. & Garavelli, M. A theoretical study of the lowest electronic states of azobenzene: the role of torsion coordinate in the cis-trans photoisomerization. *Theor. Chem. Acc.* **111,** 363–372 (2004).
42. Miyamoto, Y., Rubio, A. & Tománek, D. Real-time *ab initio* simulations of excited carrier dynamics in carbon nanotubes. *Phys. Rev. Lett.* **97,** 126104 (2006).


## Acknowledgements

Most computations were performed with the parallel computing system at AIST, whereas the long-time simulation (~500 fs) of an azobenzene molecule was performed with the Supercomputer System at the Cyberscience Center of Tohoku University. YM acknowledges support from the Joint Research Program, ending in March 2014, consisting of the Cyberscience Center in Tohoku University, Nanosystem Research Institute in AIST, and IT Platform Division in NEC Corporation. YT acknowledges financial support from KAKENHI and JST-PRESTO, and from the Strategic Programs for Innovative Research (SPIRE), MEXT, and the Computational Materials Science Initiative (CMSI), Japan.

## Author Contributions

Y.M. and N.O. performed the numerical simulations. Y.M. prepared all the figures. Y.M., Y.T. and T.O. wrote the main text. All authors reviewed the manuscript.

## Additional Information

**Supplementary information** accompanies this paper at http://www.nature.com/srep

**Competing financial interests:** The authors declare no competing financial interests.

**How to cite this article**: Miyamoto, Y. *et al.* Conservation of the pure adiabatic state in Ehrenfest dynamics of the photoisomerization of molecules. *Sci. Rep.* **5**, 18220; doi: 10.1038/srep18220 (2015).

This work is licensed under a Creative Commons Attribution 4.0 International License. The images or other third party material in this article are included in the article's Creative Commons license, unless indicated otherwise in the credit line; if the material is not included under the Creative Commons license, users will need to obtain permission from the license holder to reproduce the material. To view a copy of this license, visit http://creativecommons.org/licenses/by/4.0/